# Analysis of Failure of Crosslinked Polyethylene Cables Because of Electrical Treeing: A Physicochemical Approach

**R. Sarathi,[1] Supriyo Das,[1] C. R. Anil Kumar,[1] R. Velmurugan[2]**

[1]*Department of Electrical Engineering, Indian Institute of Technology, Madras, Chennai 600 036, India*
[2]*Composite Technology Centre, Indian Institute of Technology, Madras, Chennai 600 036, India*

Received 31 March 2003; accepted 16 December 2003

**ABSTRACT:** The present work investigated the breakdown characteristics of high-voltage crosslinked polyethylene (XLPE) cable by electrical trees under ac and composite voltages. The electrical trees resemble either a tree or a bushy structure. The importance of the Weibull parameters for the present study was emphasized. The failure zone of the XLPE cables was characterized by experimental techniques such as wide-angle X-ray diffraction, differential scanning calorimetry, and thermogravimetric–differential thermal analysis, to understand the phase constituents affected by electrical trees. The impact test and flexural test results indicate that material with high stiffness/toughness allows tree formation and causes early failure of the material. The characteristic variation of the aged XLPE cables was investigated by a dynamic mechanical analyzer (DMA). The activation energy values were calculated from the DMA data. The rate of tree propagation was found to be less for materials (XLPE) with high activation energy. © 2004 Wiley Periodicals, Inc. J Appl Polym Sci 92: 2169–2178, 2004

**Key words:** crosslinked polyethylene (XLPE); treeing; activation energy; differential scanning calorimetry (DSC); thermogravimetric–differential thermal analysis (TG–DTA)

## INTRODUCTION

Crosslinked polyethylene (XLPE) has been used as an electrical insulating material in underground distribution and transmission cables, for almost four decades because of excellent dielectric strength, low dielectric permittivity and loss factor, good dimensional stability, solvent resistance, and thermomechanical behavior. However, it is now understood that the polymers experience ageing when subjected to a stress, which may even lead to failure.[1] The life expectancy of high-voltage power cables is adversely affected by "electrical treeing," a prebreakdown phenomenon that accounts for premature failure of cables in service.[2] It is well known that electrical treeing occurs in polymeric insulation in underground cables, when subjected to high local electrical stress. With the increase in power transmission capacity, it has become necessary to design and develop a compact, cost-effective, and reliable insulation structure for underground cables. A survey of earlier work, on the failure of underground cables in service, indicates that a large body of literature is available on water treeing but the details of inception, propagation, and termination of electrical trees under different voltages are scanty.[3–7] Failure of insulation, attributed to treeing at operating voltage level, is a matter of great concern, and power supply utilities worldwide are investigating the situation. Recently, it has been shown that testing long-length cables, for defects or damage, under a composite voltage formed by ac and dc, is more reliable than the ac/dc voltage test.[8] The composite voltage helps one to understand the defects present in the insulation structure. Also, in practice, the underground cable mimics the composite stress (ac superposed with dc voltage) that arises because of trapped charges. In the present work, methodical experimental studies were carried out to understand the growth dynamics of electrical trees in underground XLPE cables under ac and composite ac and dc voltages.

The role of chemistry in the growth dynamics of electrical trees has not been studied in detail.[9] Here, certain physicochemical diagnostic tests were carried out to understand the degradation of material, ascribed to electrical tree formation, using wide-angle X-ray diffraction (WAXD), differential scanning calorimetry (DSC), and thermogravimetric–differential thermal analysis (TG–DTA). The characteristic changes in the XLPE material, attributed to ageing, were analyzed using dynamic mechanical analysis (DMA). The mechanical properties and the dynamics of the electrical trees are correlated in the present work.

*Correspondence to:* R. Sarathi (rsarathi@iitm.ac.in).

Journal of Applied Polymer Science, Vol. 92, 2169–2178 (2004)


## EXPERIMENTAL

High ac voltage at power frequencies was produced from a transformer rated at 20 kVA, 50 Hz, 20 kV. The

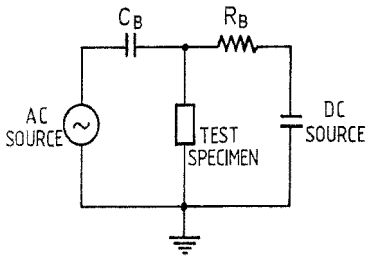


**Figure 1** Composite voltage generation circuit.

ac voltage was measured using a capacitance divider. The basic circuit used for generating the composite ac and dc voltages is shown in Figure 1. The dc voltages were measured using a resistance divider. The capacitor $C_b$ and the resistance $R_b$ serve as blocking elements to safeguard each voltage source against direct power feed from the other source. In general, it is essential to obtain the required database in a short time. For this purpose, the point from which a tree can originate has been predetermined by introducing defects of known geometry into the body. The specimens used for generation of electrical trees in the laboratory were obtained from 33-kV XLPE cable. The outer semiconducting layer of the cables was peeled off, after applying a heat pad to the surface. Samples of 2 cm length were cut from a long length of cable. The specimens were stabilized by heating them at about 90°C for 90 h. A conducting defect was simulated by inserting a sharp metallic needle into the dielectric body. The trees were expected to initiate from this point. The needle used had a nominal tip radius of curvature of 5 $\mu$m. The selected pins were inserted into the insulation at 130°C and annealed for 0.5 h to relieve the residual strain at the tip of the needle. The effective thickness between the central conductor and the tip of the electrode was maintained between 3 and 5 mm. The space between the pin and the dielectric was effectively sealed with cold setting Araldite and the specimens were immersed in filtered, degassed mineral transformer oil ready for voltage application. The needle was connected to the high-voltage source and the cable conductor was grounded. The electrode configuration used in the present work is shown in Figure 2.

The treeing studies were also carried out with samples aged under different conditions.

### Thermal ageing

The XLPE samples were placed in a temperature-controlled oven maintained at 100°C for 30 days. The oven was circulated with clean air. The initial color of the sample was white and, upon termination of the ageing, the color of the sample changed to dim yellowish orange. In the present work, this specimen is identified as Type-A material.

### Cyclic thermal stress

In this study, the XLPE samples were placed in a temperature-controlled oven maintained at 100°C for 8 h and, on removal, suddenly quenched in a distilled water bath, and kept for 30 min to allow the surface temperature of the specimen to return to room temperature. The cyclic process was continued 50 times before carrying out the experimental study. The sample color was changed to light reddish brown at the end of the ageing. The material is identified as Type-B.

To understand the influence of rapid cooling of insulation material on treeing inception and propagation, one set of samples was removed from thermal ageing, and allowed to cool for 8 h, and then cycled 50 times. The color of the material was unaltered. The material is identified as Type-C.

### Physicochemical analysis

To diagnose the characteristic change in the material attributed to treeing, certain physicochemical analysis were carried out. Also, to relate the mechanical aspects of the material to the insulation material, detailed analyses were carried out using dynamic mechanical analysis.

#### Wide-angle X-ray diffraction (WAXD)

This study helps to identify any variation in percentage of crystallinity of the material or addition of new phases in the tree, followed by the breakdown zone. Loss of crystallinity peaks is an indication of characteristic variation in the material. In the present work, WAXD measurements were done with a Philips (The Netherlands) X-ray diffractometer. A scan rate of 2°/min at 2000 cycles, using Cu–$K_\alpha$ radiation of wavelength 1.596 Å, was used. A radial scan of Bragg angle

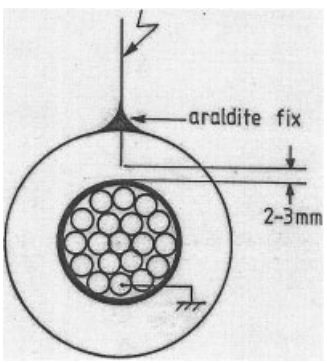


**Figure 2** Electrode configuration of the specimen.

($2\theta$) versus intensity was obtained with an accuracy of $\pm 0.25°$ at the location of the peak.

### Differential scanning calorimetry (DSC)

This technique involves the measurement of energy necessary to establish a zero temperature difference between the specimen and a reference material when the two specimens are subjected to thermal degradation. The melting behavior of the specimens was observed using a Perkin–Elmer model DSC-2C apparatus (Perkin Elmer Cetus Instruments, Norwalk, CT). The experiments were performed in a nitrogen atmosphere, at a heating rate of 10°C/min. Alumina was used as a standard.

### Thermogravimetric–differential thermal analysis (TG–DTA)

The TG–DTA study was carried out with Netzsch STA 409C equipment (Netzsch-Gerätebau GmbH, Bavaria, Germany). The experiments were performed in a nitrogen atmosphere, in the range 25 to 1200°C, at a heating rate of 20°C/min. Alumina was used as a standard catalyst. The TG and DTA methods are very effective techniques to study the chemical and physical phenomenon as a function of temperature.

### Dynamic mechanical analysis (DMA)

Viscoelastic measurements of both storage shear modulus and mechanical loss tangent were performed on a TA Instruments DMA-983 viscoelastimeter (TA Instruments, New Castle, DE) using a three-point bending method. Experiments were carried out over a wide frequency range (2, 5, 10, and 25 Hz) in the temperature range 30–90°C under controlled sinusoidal strain, at a heating rate of 2°C/min, under a flow of nitrogen. All experiments were performed on a $60 \times 10 \times 4$-mm rectangular strip at different frequencies. The viscoelastic properties, such as storage modulus ($E'$) and mechanical loss tangent (tan $\delta$), were recorded as a function of temperature and frequency. Dynamic mechanical analysis, over a wide range of temperature and frequencies, permits determination of the viscoelastic behavior of molten polymers and provides valuable insight into the relationship between structure, morphology, and physical properties of polymeric matrices.

### Flexural test

The ability of a material to resist deformation under load is its flexural strength. For materials that do not break, the load at yield, typically measured at 5% deformation/strain of the outer surface, is the flexural strength or flexural yield strength. By carrying out the flexural test, it is possible to understand the variation of characteristics of the XLPE material used in the present work. The test was carried out in an Instron 4301 universal testing machine (Instron, Canton, MA) of 500 kg capacity. The pulling speed during the test was maintained at 5 mm/min.

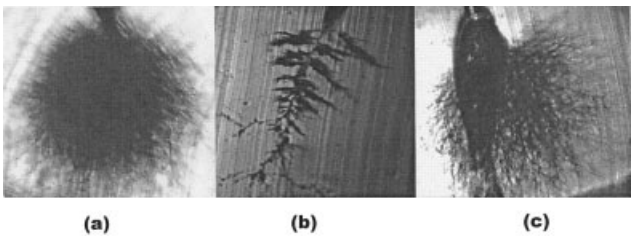


**Figure 3** Electrical trees under ac voltage: (a) bush-type tree; (b) treelike tree; (c) tree followed with breakdown.

### Impact test

This test was carried out in a Frank model machine of 50-J maximum capacity (Karl Frank GmbH, Germany; Type 53568). Important factors that affect the toughness of a structure include low test temperatures, extra loading, and high strain rates attributed to wind or impacts and the effect of stress concentrations such as notches and cracks. Here, the impact test was carried out to understand the material properties ascribed to ageing of the material.

## RESULTS AND DISCUSSION

The process of tree inception and propagation followed by breakdown in an insulation structure is a highly complicated process. Under normal operating voltage stress, a series of partial prebreakdown channels emanates from a defect site present in the form of gas cavities, or conducting inclusions or intrusions, in the insulation structure. Depending on the size and shape of the defect, the stress distribution in the insulation structure is altered, causing joule heating/oxidation of the material and a reduction in breakdown strength/local erosion forming prebreakdown channels. These channels, formed around the defect site in the dielectric structure, resemble branches of a tree and thus the term "treeing" is given to the deleterious process; and, because such an occurrence is purely a consequence of electrical stress, the mechanism is termed "electrical treeing."

Figure 3 shows typical optical photographs of different types of electrical trees formed in the XLPE cable specimen under high voltages. A bush-type of tree [Fig. 3(a)] and a treelike tree [Fig. 3(b)] structure are formed at the tip of the needle electrode, connected to high voltages. Figure 3(c) shows a typical breakdown path formed in the insulation structure

attributed to propagation of electrical trees terminating at the ground electrode. Under ac voltages, both treelike and bush-type trees were observed.

When high voltage is applied to an insulation structure, the local electrical field near the defect site is enhanced. If the order of magnitude exceeds the maximum electric field strength of the material, incipient damage occurs near the defect site. Further, injected charges from the high-voltage electrode to the insulation structure are trapped near the defect site formed and the charges are deposited in the surface of the damaged zone. This causes a local reaction with the applied field and reduces the electric field in the zone. The decomposition products of the insulating materials subject to discharges are mainly gaseous, although unsaturated hydrocarbons and conducting carbons are also produced.[10] In general, the electronegativity, and the chemical reactivity of the gas contained in the defect zone, can retard or accelerate tree growth. Sometimes, the charges were injected into the insulation structure through the defect-formed zone-enhancing field, causing further enlargement of the channel resulting in the "treelike tree" structure. Otherwise local discharges occur, causing increased diameter of the damage zone and forming the "bush-type" of electrical tree. Some authors suggest that channel propagation will continue, provided there is a critical energy stored at the tip of the channel allowing degradation of the material by discharges. If there is not sufficient energy, the channel will stop growing and discharge will recur in the main branches forming a bush-type tree structure.[11] Shimizu et al.[12] explained that the inception of trees is attributed to injected charge, and propagation occurs by chain scission forming free radicals. The process is aided by the presence of oxygen in the medium. In general, the reaction kinetics, responsible for the formation of free radicals, is as follows, and the process confirms that treeing is a degradation process:

$$\mathrm{RH} \xrightarrow{\text{Homolytic splitting}} \underset{\text{(Free radical)}}{\mathrm{R}^*} + \mathrm{H}^* \quad (1)$$

When the free radical reacts with oxygen, an autooxidation process starts. The free radical reacts with oxygen to form hydroperoxide. The unstable hydroperoxide decomposes and reproduces the free radical. The repetition of the process breaks the polymer chain R′ and the degradation process follows.

$$\mathrm{R}^* + \mathrm{O_2} \xrightarrow{\text{Oxidation}} \mathrm{ROO}^* \text{ (alkyl peroxy radical)} \quad (2)$$

$$\mathrm{ROO}^* + \mathrm{RH} \rightarrow \mathrm{ROOH} + \mathrm{R}^* \text{ (free radical)} \quad (3)$$

$$\mathrm{ROOH} \rightarrow \mathrm{RO}^* + \mathrm{OH} \quad (4)$$

By the chain-scission process

$$\mathrm{RO}^* + \mathrm{R'—CH_2—R}^* \rightarrow \mathrm{RH} + \mathrm{R'—CH{=}O} + \mathrm{R}^* \quad (5)$$

The applied electric field and the local medium determine the size and shape of the electrical tree structure in the insulation.

In the present work, 20 identical samples were used for the study, and the needle electrodes were connected to the high voltage. The study was carried out at different voltage levels and the time to breakdown was noted. In the present study, censored data analyses were used. Only 10 failure times were noted and the remaining samples were cut and examined for any tree structures. The unfailed samples were found with tree structures (especially in the samples stressed at lower voltages), whereas at high voltages, no clear-cut tree structures were noticed. The reason for this is that the injected charges cause reaction at some point surrounding the pin electrode, initiating the tree to form quickly and reach the ground electrode-causing breakdown. At low-voltage magnitudes, the injected electrons do not attain sufficient energy to cause splitting of material and only local damage will occur, increasing the diameter of the defect. We thus conclude that the bush type of tree structures is less dangerous than the treelike tree structures, where the rate of tree propagation is aided by the applied voltage.

Even though the samples are identical, the scatter in the failure times of the specimens is large. It is essential to use statistical tools to understand the severity attributed to electrical stress. The cumulative Weibull distribution function is given by

$$F(t) = 1 - \exp\left[-\left(\frac{t}{\tau}\right)^{\beta}\right] \quad (6)$$

where $\tau$ is the scale parameter; $\beta$ is the shape parameter; and $t$ is the random variable, usually time to breakdown. $F(t)$ indicates the proportion of specimens tested that will fail by time $t$. The scale parameter $\tau$ represents the time required for 63.2% of tested units to fail. The shape parameter $\beta$ is a measure of dispersion of failure times for $t = \tau$. The unit of $\tau$ is time in minutes and beta is a dimensionless number. The life of an insulation material could be assessed by a test in which the solid dielectric is subjected to a constant high-voltage stress until failure. Repeating the test several times on identical specimens usually yields greatly varying values of times. These values can be represented statistically by the Weibull distribution.[13] The experimental data are used to estimate the parameters of the distribution. Figure 4 shows a typical

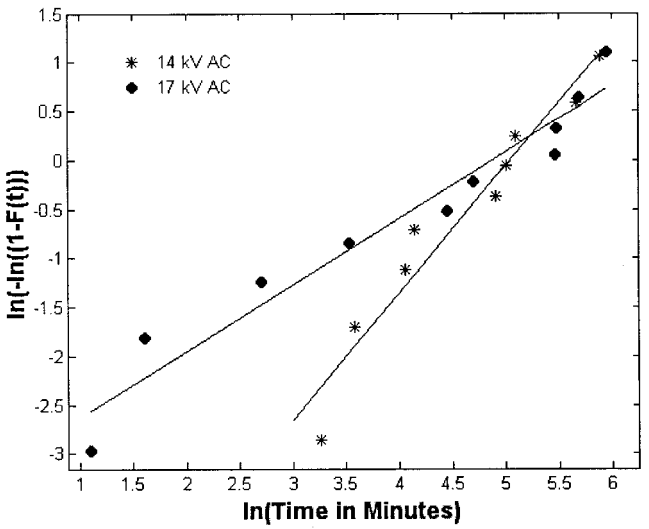


**Figure 4** Weibull plot of times to failure of XLPE specimen attributed to electrical tree under ac voltage.

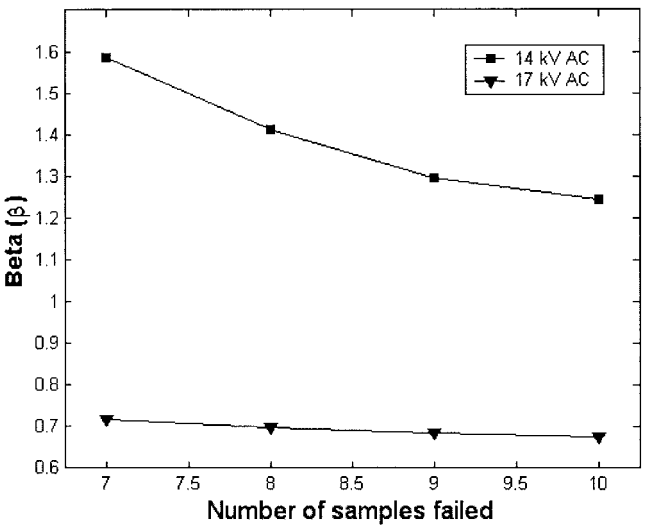


**Figure 5** Variation in the shape parameter ($\beta$) with number of samples failed.

Weibull plot for the failure times of the insulation structure attributed to electrical trees, operated at different voltage levels under ac voltages. Table I shows the variation in the characteristic life ($\tau$) of the insulation material, and the shape parameter ($\beta$), for the failure data caused by electrical treeing, at different voltage profiles. In the case of aged specimens, it is observed that the characteristic life of this insulation material, ascribed to electrical treeing, is much higher than that of the virgin specimen. Also the values of beta for the aged specimens are almost the same, which indicates that the mechanism of failure is almost the same. The cause of increase in the characteristic life of the material could be attributable to increase in the packing density, thereby reducing the charge-trapping sites.

Under composite voltages, an increase in the dc bias voltage increases the failure time of the insulation structure attributed to electrical treeing, irrespective of the polarity of the dc bias voltage. The variation in failure time, under composite voltage and ac voltage, is mainly the result of space charge accumulation in the XLPE material. It is well known that the charge-trapping sites in the XLPE material are in the noncrosslinked part, additives, and residual byproducts formed during manufacturing. Liu et al.,[14] observed that the tree inception voltage is less under positive dc voltage than under negative dc voltage. Under the composite voltages, superposing positive or negative dc voltage on ac voltage causes the zero level to float with respect to ground, and the voltage waveshape is unipolar in nature. The space charge field, formed in the bulk volume of the insulation, opposes the applied electric field. When the applied electric field is added to the space charge field in the zone then, if the effective field exceeds the breakdown strength of the material, a tree is formed. Under ac voltages, both treelike and bush-type trees are formed. Under the composite voltages, irrespective of the dc voltage magnitude and polarity, a bush type of tree is observed. When the tree propagates, the trapped charges react locally and cause local degradation, forming a bush-type tree structure.

**TABLE I**
**Variation in Characteristic Life ($\tau$) of the Material and the Shape Parameter ($\beta$) for Different Materials**

| Material | Voltage magnitude | Characteristic time ($\tau$) (min) | Shape parameter $\beta$ |
|---|---|---|---|
| Virgin | 14kV AC | 155 | 1.30 |
| Virgin | 14 kV AC + 5 kV DC | 121 | 1.13 |
| Virgin | 14 kV AC + 7 kV DC | 147 | 1.05 |
| Virgin | 14 kV AC − 5 kV DC | 157 | 1.01 |
| Virgin | 14 kV AC − 7 kV DC | 199 | 1.00 |
| Type-A | 14 kV AC | 1408 | 1.05 |
| Type-B | 14 kV AC | 445 | 1.02 |
| Type-C | 14 kV AC | 1274 | 1.01 |

In addition, the slope parameter ($\beta$), obtained under different electrical stresses, varies. It is clear that, if $\beta > 1$, the failure of the insulation materials is the result of local erosion. When the electrical stress is high, $\beta < 1$, and causes intrinsic failure (puncture) of the insulation structure. Initially, with a certain number of samples, the slope parameter is >1 and, when the number of failure of samples increases, the value of $\beta$ is reduced, as shown in Figure 5. Similar characteristics were observed by Bozzo et al.,[15] showing a reduction in the $\beta$ values with respect to time. This clearly indicates that, in the specimen that is stressed for a long time, especially in the electrical tree-formation studies, the failure of the specimen is attributed not only to the electrical stress but also to local conditions, which alter the failure rate and cause early failure of the material.

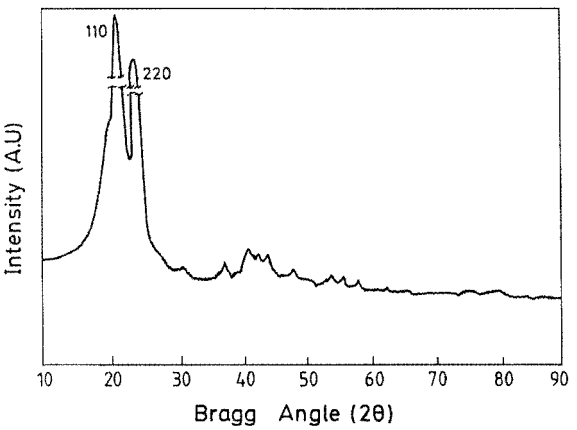


**Figure 6** WAXD pattern of XLPE specimen.

Carrying out experimental studies and understanding the failure times alone is not sufficient. It is essential to understand the characteristic changes that occur in the tree-forming zone using physicochemical analysis. The local electric discharges cause considerable changes in the structure of the material. Among other things, carbonization, chain scission, and conversion of amorphous to crystalline phase are known to occur. The X-ray diffraction pattern of virgin XLPE material, and the treeing followed by breakdown, are very similar, and for the sake of brevity only the virgin XLPE sample WAXD is shown in Figure 6. Andjelkovic et al.[16] carried out accelerated ageing of XLPE cables in the laboratory and studied the change in percentage of crystallinity attributed to ageing. The WAXD plot of the XLPE specimen showed two peaks at 21.5 and at 23.9°, which are characteristic of the 110 and 220 lattice planes.[17] The percentage of crystallinity of the material was calculated using Hinrichsen's method,[18] which for XLPE material is 56. The WAXD spectrum does not appear to show any change in the position of the peaks, or in their splitting throughout the scan range, except for a minor variation in the intensity of the peaks. This means that hardly any change has occurred in the percentage of crystallinity of the material, nor is there any new phase.

A diagnosis of the treed zone was made using a differential scanning calorimeter. The DSC thermogram of the XLPE specimen is shown in Figure 7. A reduction in the melting point of the material in the treed zone is observed. No new phase was observed, which was confirmed by similar thermograms obtained for the virgin and the degraded (treed) samples.

The thermal behavior of the material, attributed to ageing, was characterized using TG–DTA studies. Figure 8 shows the TG and DTA thermograms of the XLPE material aged under different conditions. In a nitrogen atmosphere, the TG curve for XLPE material shows a gradual weight loss above 320°C. The derivative curve shows that weight loss occurs especially at 467°C. Similar characteristics were observed for all the aged specimens. The DTA spectra of the virgin material indicate endothermic peaks at 106, 507, and at 665°C. The exothermic peaks are observed at 422 and at 618°C. The DTA spectra of the aged specimens show considerable variation compared to the virgin material, which indicates that ageing altered the basic thermal characteristics of the material.

To further understand the differences in the virgin and types A, B, and C specimens, flexural test were carried out. The results, shown in Table II, indicate that ageing of the material reduces the elongation; the higher the elongation, the higher the stiffness of the material. The impact test results (notched and unnotched), also shown in Table II, indicate that thermally aged material is tough compared to virgin and other types of aged materials. When the material absorbs high energy, we consider that the material is tough. Comparing the treeing failure time, flexural test data, and the impact test results of the material, it could be concluded that material with high stiffness/toughness allows tree formation and causes early failure of the material.

Figure 9(a) shows the variation in storage modulus of the XLPE specimen at different temperatures. Ageing alters the storage modulus of the material. Figure 9(b) shows the variation in the tan δ of the XLPE specimen at different temperatures. It is clear that a characteristic change has occurred in the material because of ageing. Reduction in tan δ of the material is advantageous for any insulation material. Comparing the values of tan δ and the characteristic life of the material in Table I, high tan δ implies a high rate of tree propagation.

Figure 10(a) shows the variation in storage modulus of XLPE specimen at different temperatures, measured at different frequencies. As the frequency increases, the storage modulus increases. Similar characteristics were also observed for the aged specimens. The storage modulus is higher for the virgin sample than for the aged material. Figure 10(b) shows the variation in the tan δ at different temperatures for

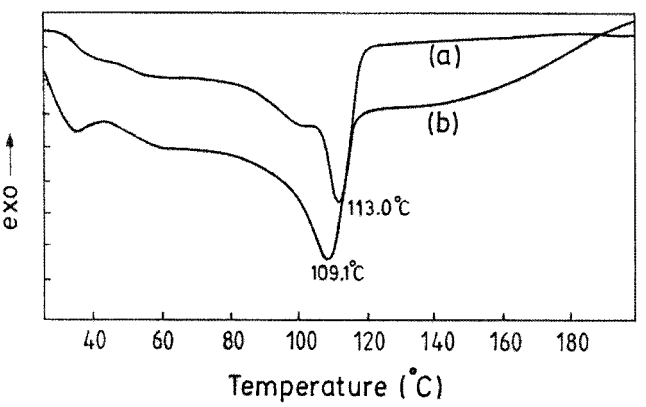


**Figure 7** DSC thermograms: (a) virgin sample; (b) tree followed with breakdown zone sample.

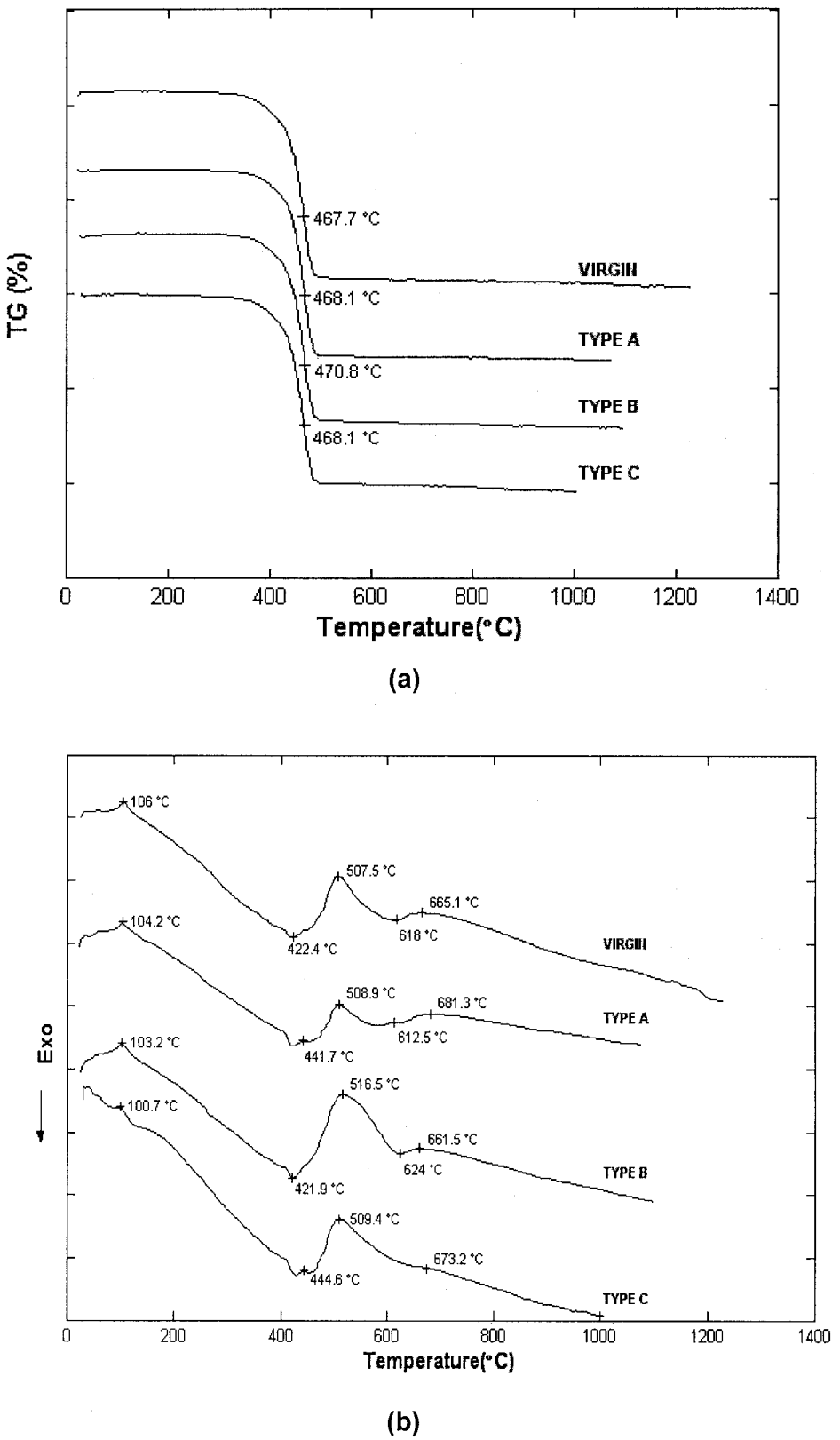


**Figure 8** TG–DTA spectra of XLPE material: (a) TG spectra; (b) DTA spectra.

**TABLE II**
**Impact Test and Flexural Test Results**

| Sample type | Impact test (Izod) | | Flexural analysis | |
|---|---|---|---|---|
| | Unnotched (J) | Notched (J) | Load (kg) | Elongation (mm) |
| Virgin | 1.1 | 1.0 | 1.396 | 13.2 |
| Type-A | 0.85 | 0.65 | 1.973 | 12.32 |
| Type-B | 1.05 | 0.80 | 1.57 | 13.05 |
| Type-C | 0.9 | 0.75 | 1.852 | 12.94 |

different frequencies for the virgin material. Tan δ, which is a dimensionless parameter, is a measure of the ratio of energy lost to the energy stored in a cyclic deformation. It is the loss tangent that is high for low frequencies measured at low temperatures and the converse when the values are measured at high temperature, in the range studied. The relaxation peak temperature is increased by about 15°C when the frequency is increased from 2 to 25 Hz, especially for the virgin material. This characteristic variation is limited

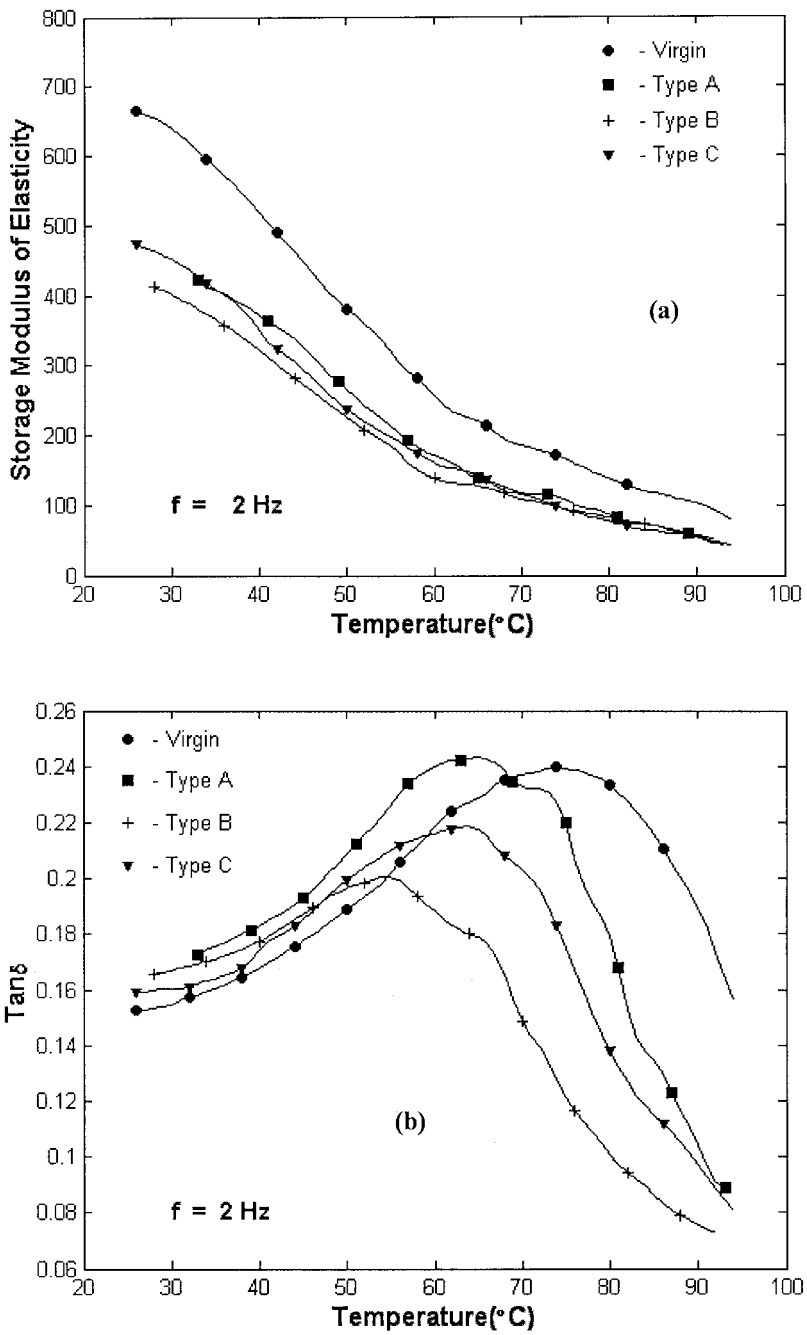


**Figure 9** (a) Plot of storage modulus of XLPE material as a function of temperature; (b) plot of tan δ as a function of temperature.

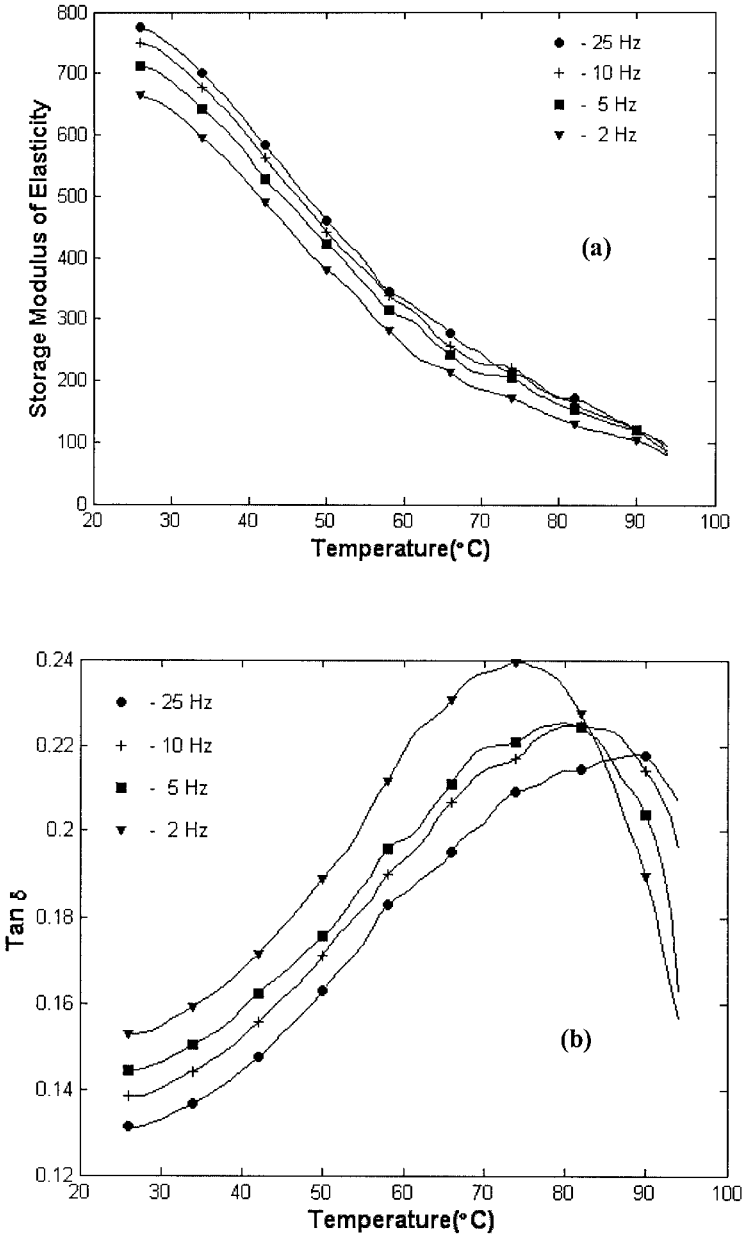


**Figure 10** (a) Plot of storage modulus of XLPE material as a function of temperature at different frequencies; (b) plot of tan δ as function of temperature at different frequencies.

to 5°C in all the aged specimens used here. It is possible to relate the temperature at which the relaxation process is observed, and the frequency of excitation ($f$), by the Arrhenius equation[19]

$$f = f_0 \exp\left[\left(\frac{-E_a}{RT}\right)\right] \tag{7}$$

where $f_0$ is a constant, $f$ is the frequency of the test, $R$ is the gas constant, and $E_a$ is the activation energy for the relaxation process. According to the above equation, a plot of log $f$ versus $1000/T$ should give a straight line with a slope that is directly related to the apparent activation energy for the relaxation process of the material, and is shown in Figure 11. Calculated activation energies are shown in Table III. Comparing the activation energy and the failure time of material resulting from electrical trees, higher activation energy yields a reduction in propagation rate of the electrical trees, which correlates with an increase in the failure time attributed to treeing.

## CONCLUSIONS

Electrical treeing causes early failure of electrical insulation structures under normal operating condi-

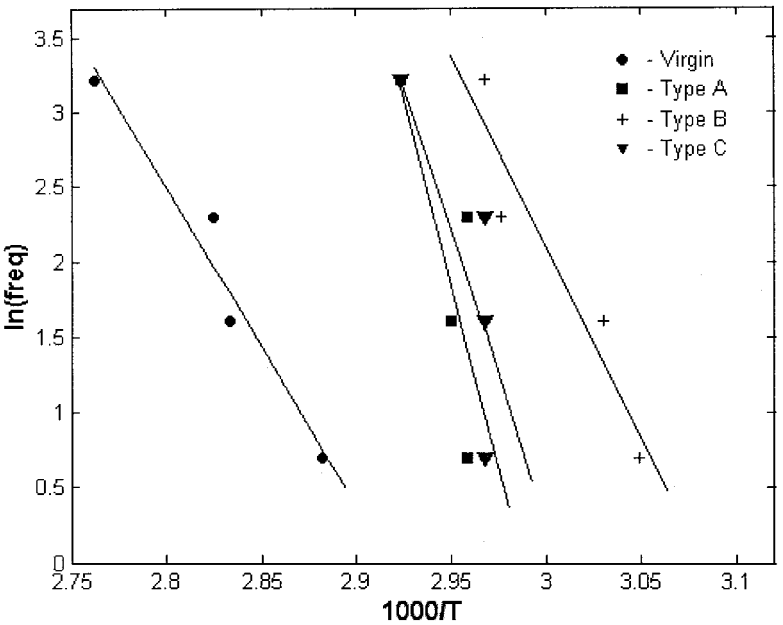


**Figure 11** Calculation of activation energy.

tions. Either a treelike or a bush-type tree structure can form from a defect site. The characteristic life of the insulation material is reduced when composite voltages are formed by ac voltage superposed over positive dc voltage. In the Weibull distribution parameter study, estimation of the beta factor helps one understand the failure rate in the insulation structure under different voltage profiles.

Physicochemical analyses, especially the WAXD and DSC results, show that no additional phases are formed in the treed zone. A slight reduction in the melting point of the insulation structure is observed with the treed zone. The reaction kinetics show the formation of free radicals in the XLPE specimen in the treed zone and shows that treeing is a degradation process. The presence of oxygen in the zone accelerates the process of degradation of the material. The TG analysis indicates that major degradation occurs at around 478°C in XLPE material. The DTA results confirm that the material properties are altered as a consequence of ageing of the material. The impact test and flexural test results indicate that the material with high stiffness/toughness allows tree formation and causes early failure of the material. The DMA test results show that ageing alters the storage modulus and tan $\delta$ of the material. It thus may be concluded that an increase in the activation energy of the material reduces the rate of tree propagation.

**TABLE III**
**Activation Energy of the Materials**

| Sample type | Activation energy (kJ/mol) |
|---|---|
| Virgin | 177.17 |
| Type-A | 420.52 |
| Type-B | 248.21 |
| Type-C | 322.69 |

## References

1. Dissado, L. A.; Fothergill, J. C. Electrical Degradation and Breakdown in Polymers; Peter Peregrinus: London, 1992.
2. Eichhorn, R. M. IEEE Trans Elect Insul 1976, EI-12, 2.
3. Densley, R. J. IEEE Trans Elect Insul 1979, EI-14, 148.
4. Ieda, M. IEEE Trans Elect Insul 1980, EI-15, 206.
5. Noto, F.; Yoshimura, N. IEEE Trans Elect Insul 1986, EI-21, 889.
6. Tanaka, T. IEEE Trans Dielect Elect Insul 2001, 8, 733.
7. Steennis, E. F.; Kreuger, F. H. IEEE Trans Elect Insul 1990, 25, 989.
8. Grzybowski, S.; Fan, J. In: Proceedings of the 5th International Conference on Properties and Application of Dielectric Materials, Seoul, Korea, May 25–30, 1997; No. 05052.
9. Dissado, L. A. IEEE Trans Dielect Elect Insul 2002, 9, 483.
10. Laurent, C.; Mayoux, C. IEEE Trans Elect Insul 1980, EI15, 33.
11. Olyphant, M. IEEE Trans Power Apparat Syst 1963, IEEE-PAS-69, 1106.
12. Shimizu, N.; Horii, K. IEEE Trans Elect Insul 1985, EI-20, 561.
13. Nelson, W. Applied Life Data Analysis; Wiley: New York, 1982.
14. Liu, Z.;, Liu, R.-S.; Wang, H.; Liu, W. IEEE Trans Elect Insul 1989, 24, 83.
15. Bozzo, R.; Guastavino, F.; Cacciari, M.; Contin, A.; Montanari, G. C. In: Conference Record of the 1994 IEEE International Symposium on Electrical Insulation, Pittsburgh, PA, June 5–8, 1994; pp. 269–272.
16. Andjelkovic, D.; Rajakovic, N. Elect Eng 2001, 83, 83.
17. Agarwal, S. L. J Polym Sci 1955, 18, 17.
18. Nath, R.; Perlman, M. M. IEEE Trans Elect Insul 1989, EI-24, 409.
19. Heijboar, T. In: Molecular Basis of Transitions and Relaxations; Meier, D. J., Ed.; Gordon & Breach: New York, 1978; p. 5.